Energy spectrum of layered semiconductors in a magnetic field parallel to the layers: Voigt geometry

K. H. Yoo[1,*] and L. R. Ram-Mohan[2,3]
[1]*Department of Physics and Research Institute for Basic Sciences, Kyung Hee University, Seoul 130-701, Korea*
[2]*Department of Physics, Worcester Polytechnic Institute, Worcester, Massachusetts 01609, USA*
[3]*Department Electrical and Computer Engineering, Worcester Polytechnic Institute, Worcester, Massachusetts 01609, USA*
(Received 16 July 2010; published 23 November 2010)

The electronic band structure of zinc-blende layered semiconductor heterostructures is investigated theoretically in the presence of an in-plane magnetic field, a configuration we label as the Voigt geometry. We use a Lagrangian formulation for modeling the band structure in the individual layers within the $\mathbf{k}\cdot\mathbf{P}$ model. This approach has been shown by us to provide the correct ordering of the derivatives appearing in the multiband description of Schrödinger's equations for the envelope functions through the application of the principle of stationary action. Finite element modeling of the action integral provides a natural and efficient approach to the inclusion of in-plane magnetic fields in the energy-level analysis. Calculations for quantum wells and superlattices are presented, and the complex energy-level structure obtained for the layered structures.

DOI: 10.1103/PhysRevB.82.195327 PACS number(s): 78.67.−n, 78.20.Bh, 78.30.Fs

I. INTRODUCTION

A uniform magnetic field changes the energy levels of charged carriers in a physical system in an intrinsic, fundamental way,[1] so that it provides a nondestructive perturbation of the electronic energy levels in a physical material. For this reason, an externally applied magnetic field has been used as a controlled perturbation in the investigation of the electronic energy levels in quantum systems. For example, magneto-optics has been used on bulk semiconductors for the determination of effective masses of free carriers in the conduction and the valence energy bands.[2–5] Magneto-optical spectroscopy was extended to narrow energy band-gap materials, again to investigate the properties of electrons and holes in bulk materials, and a full eight-band model was developed[6–9] based on an extension of the Luttinger treatment of the valence band (VB) in the presence of a magnetic field.[10,11]

In layered quantum semiconductor structures, the theoretical description of energy levels of free carriers in the structures in a magnetic field perpendicular to the layers has been thoroughly investigated.[12–15] For example, the elucidation of the band structure of HgTe/CdTe superlattices with the help of magneto-optical experiments provided a detailed explanation of the variation in the energy bands and also of the changes in the effective masses of carriers in the superlattices with varying layer thicknesses.[16–21] We label this magnetic field configuration, with the magnetic field perpendicular to the layers, as the "Faraday geometry" since for the typical optical experiment the incoming radiation is incident parallel to the magnetic field. The electronic states are expressed as a product of Landau orbits in the plane of the layers and an envelope function that is dependent on the coordinate of the growth direction. Within the framework of an eight-band model, the coupled Schrödinger equations are solved by including the interaction energy between the external field and the dipole moment of the electron due to orbital motion in the field, and also the interaction energy for the spin magnetic moment of the electron interacting with the external magnetic field.

In this paper, we consider the theoretical determination of the energy levels in layered quantum semiconductor heterostructures in an external magnetic field that is parallel to the layers. We refer to this configuration as the "Voigt geometry" with the incident radiation normal to the layers and to the applied magnetic field in magneto-optical experiments. We work in the envelope function approximation[22–25] in an eight-band model with the conduction (CB), and the valence heavy-hole, light-hole, and the split-off energy bands including spin. In this geometry, with the Landau orbits in general crossing the planar heterostructure interfaces, the boundary conditions satisfied by the electronic wave functions are substantially more complex than those for the Faraday geometry where the orbits are considered to reside in the layers. We show here that the issues of the coupled equations and the boundary conditions are readily treated by employing the finite element method (FEM) for the numerical work.[26–31]

The Voigt geometry magneto-optics was considered earlier essentially in a one-band (CB) picture both experimentally and theoretically by Maan[32–35] and by Xia.[36,37] Altarelli and co-workers[38–40] gave a solution for the Landau states in terms of confluent hypergeometric functions, a solution that arises from the need to represent a quantum oscillator wave function over the finite domain of a given layer. In this finite domain both types of Hermite oscillator functions are needed to develop a solution. Here, we provide a more direct line of attack using the FEM.

In Sec. II, we set up an action integral approach to the evaluation of the electronic states in layered semiconductors. We have simplified our presentation considerably by restricting ourselves to a one-band model since we have already shown that operator ordering is unambiguously included in the context of the eight-band $\mathbf{k}\cdot\mathbf{P}$ model through Löwdin perturbation theory.[41] The current conservation at interfaces of the layers is obtained from the gauge variation in the Lagrangian and this condition is readily implemented in the discretized action in the FEM. Here we describe the effect of including the in-plane magnetic field in one-band model and extend it to the multiband model. Example calculations using

the full eight-band model are given in Sec. III, and the conclusions are presented in Sec. IV.

II. THEORETICAL FORMALISM

A. One-band model

We start with an electron moving in a potential $V(\boldsymbol{r})$ to show the essence of the Lagrangian approach and the effect of the magnetic field. The Schrödinger equation for the electron without a magnetic field is

$$\left[\frac{\boldsymbol{p}^2}{2m}+V(\boldsymbol{r})\right]\psi(\boldsymbol{r})=\left[-\frac{\hbar^2}{2m}\nabla^2+V(\boldsymbol{r})\right]\psi(\boldsymbol{r})=E\psi(\boldsymbol{r}). \quad (1)$$

In the Lagrangian approach, the corresponding Schrödinger action is written as

$$\mathsf{A}=\int dt\int d^3r\mathcal{L}=T\int d^3r\psi^*(\boldsymbol{r})\left[\overleftarrow{\nabla}\cdot\frac{\hbar^2}{2m}\vec{\nabla}+V(\boldsymbol{r})-E\right]\psi(\boldsymbol{r}), \quad (2)$$

where the energy E may be viewed as the Lagrange multiplier for the normalization condition. The derivative operators $\overleftarrow{\nabla}$ and $\vec{\nabla}$ act on functions to the left and to the right, respectively. In the time-independent picture investigated here, the integration over time leads to a factor T. It is easy to see that the variation in the action with respect to $\psi^*(\boldsymbol{r})$ yields the usual Schrödinger equation, Eq. (1).

We now introduce an applied magnetic field $\mathbf{B}=B_o\hat{z}$ and work in the Landau gauge[1] $\mathbf{A}=(0,B_ox,0)$. The momentum operator $\mathbf{p}$ is replaced by the minimal gauge substitution $(\mathbf{p}+|e|\mathbf{A}/c)$ so that

$$\mathbf{p}\Rightarrow\left(p_x,p_y+\frac{|e|}{c}B_ox,p_z\right). \quad (3)$$

Then the Schrödinger Lagrangian $\int d^3r\mathcal{L}=\mathsf{A}/T$ becomes

$$\int d^3r\mathcal{L}=\int d^3r\psi^*(\boldsymbol{r})\left[\overleftarrow{\nabla}_B\cdot\frac{\hbar^2}{2m}\vec{\nabla}_B+V(\boldsymbol{r})-E\right]\psi(\boldsymbol{r}), \quad (4)$$

where

$$\overleftarrow{\nabla}_B=\left(\overleftarrow{\partial}_x,\overleftarrow{\partial}_y-i\frac{|e|}{\hbar c}B_ox,\overleftarrow{\partial}_z\right) \quad (5)$$

and

$$\vec{\nabla}_B=\left(\vec{\partial}_x,\vec{\partial}_y+i\frac{|e|}{\hbar c}B_ox,\vec{\partial}_z\right), \quad (6)$$

act on functions to the left and to the right, respectively. Again the variation in the Lagrangian with respect to $\psi(\boldsymbol{r})$ yields the usual Schrödinger equation in a magnetic field

$$\left\{-\left(\frac{\hbar^2}{2m}\right)\left[\partial_x^2+\left(\partial_y+i\frac{|e|}{\hbar c}B_ox\right)^2+\partial_z^2\right]+V(\boldsymbol{r})\right\}\psi(\boldsymbol{r})=E\psi(\boldsymbol{r}). \quad (7)$$

We now move on to the layered structure. Since the magnetic field $\mathbf{B}=B_o\hat{z}$ is in the layer, we choose the growth direction to be the x axis. In the one-band model the periodic Bloch functions $u_{nk}(\boldsymbol{r})$ can be laid aside so that

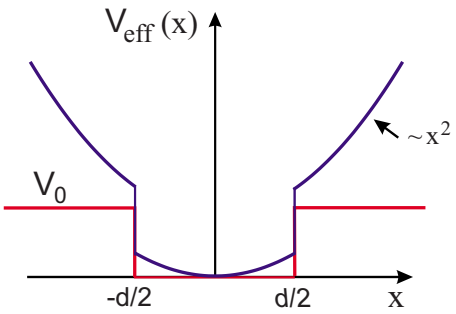

FIG. 1. (Color online) The effective potential experienced by an electron in a quantum well with an in-plane magnetic field is shown. The rectangular potential of the quantum well has a quadratic diamagnetic potential superposed on it. The orbit center is located at the center of the well for this figure.

$$\psi(\boldsymbol{r})=F(\boldsymbol{r})u_{nk}(\boldsymbol{r}),$$

$$F(\boldsymbol{r})=f(x)\exp(ik_yy+ik_zz), \quad (8)$$

and an effective mass m^* is introduced to include the influence of the other bands. The potential $V(\boldsymbol{r})=V(x)$ is the band offsets between materials. The Schrödinger Lagrangian in Eq. (4) is now

$$\int dx\mathcal{L}=\int dxf^*(x)\left[\overleftarrow{\partial}_x\frac{\hbar^2}{2m^*}\vec{\partial}_x+\frac{|e|^2B_o^2}{2m^*c^2}\left(x+\frac{\hbar c}{|e|B_o}k_y\right)^2+\frac{\hbar^2k_z^2}{2m^*}+V(x)-E\right]f(x). \quad (9)$$

The Landau orbit radius R_o is given by $R_o^2=(\hbar c/|e|B_o)$. The quantity $R_o^2k_y$ can be interpreted as the orbit center and is denoted in the following by x_o. This x_o and k_z may serve as quantum numbers in the Voigt geometry. We observe that the electron is in the effective potential

$$V_{\text{eff}}(x)=V(x)+\frac{|e|^2B_o^2}{2m^*c^2}(x+x_o)^2 \quad (10)$$

and this effective potential is sketched in Fig. 1 for a quantum well with the orbit center x_o at the center of the well.

In the FEM,[26–31] we directly evaluate the Lagrangian $\int dx\mathcal{L}$. The physical range of the layered structure along x is further subdivided in each layer into elements in each of which we approximate the envelope function $f(x)$ by local polynomials extending over the element. By minimizing the Lagrangian with respect to the coefficients of the polynomial f_j, we get a generalized matrix eigenvalue problem of the form

$$\boldsymbol{K}_{ij}f_j=E\boldsymbol{B}_{ij}f_j. \quad (11)$$

The matrix $\boldsymbol{K}$ is in general Hermitian, while the overlap integral $\boldsymbol{B}$ is real, except for superlattices. This generalized eigenvalue problem[42] is solved by standard matrix packages such as the Lanczos-Arnoldi algorithm.[43]

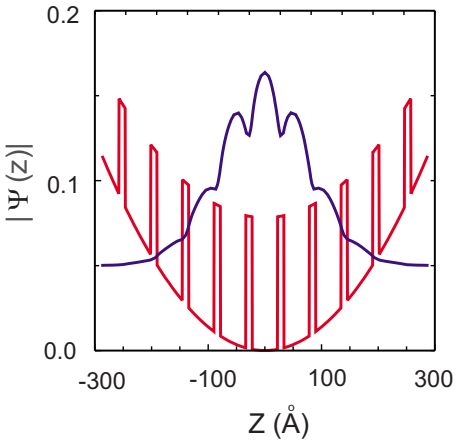

FIG. 2. (Color online) The ground state of an electron in a superlattice with an in-plane magnetic field is shown. The orbit center is placed at the center of one of the wells.

In a layered system the effective mass m^* varies with the layer and is x dependent. Therefore it is important to position $m^*(x)$ in its proper place between $\vec{\partial}_x$ and $\vec{\partial}_x$, and the Lagrangian formalism, Eq. (9), does this in a natural manner. Following Gell-Mann and Levy,[44] we substitute $f(x) \Rightarrow e^{i\Lambda(x)} f(x)$ in Eq. (9), and develop a variation in the Lagrangian density with respect to the gauge function $\Lambda(x)$. The conserved current is obtained as

$$\mathcal{J} = \frac{1}{\hbar}\left\{\frac{\delta \mathcal{L}}{\delta[\partial_x \Lambda(x)]}\right\}\Bigg|_{\Lambda=0} = \frac{\hbar}{2i}\left\{f^*(x)\frac{1}{m^*(x)}\left[\frac{d}{dx}f(x)\right] - \left[\frac{d}{dx}f^*(x)\right]\frac{1}{m^*(x)}f(x)\right\}. \tag{12}$$

With the continuity of the envelope function we now include the continuity of the conserved current by requiring the continuity of the "mass derivative"

$$\left[\frac{1}{m^*(x)}f'(x)\right]_{0^-} = \left[\frac{1}{m^*(x)}f'(x)\right]_{0^+}, \tag{13}$$

across the layer interfaces. The continuity conditions of $f(x)$ and its mass derivative can be easily implemented in the FEM.[26] An example of a calculated wave function is shown in Fig. 2 for a ground state in a superlattice with x_o at the center of one of the wells.

B. Standard eight-band model

The above discussions can be extended to the standard eight-band model by executing the Löwdin perturbation theory[41] starting from Eq. (4). The details of the multiband model without magnetic field have been given by us earlier.[45] Instead of repeating the lengthy derivation, we limit ourselves to showing explicitly the final 8×8 matrix elements for the Lagrangian density $\mathcal{L}$ in the Appendix. Again we emphasize that the Lagrangian approach keeps the correct order of operators so that the Burt-Foreman[46,47] boundary conditions are obtained in a natural manner. The Lagrangian density is of the form

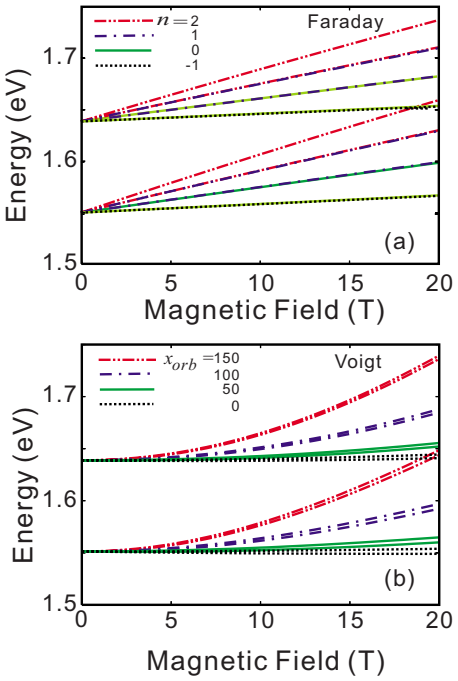

FIG. 3. (Color online) Conduction subband dispersion are shown for a 100 Å $GaAs/Al_{0.3}Ga_{0.7}As$ quantum well in a magnetic field (a) in the Faraday geometry for Landau quantum numbers −1, 0, 1, and 2; and (b) in the Voigt geometry for the orbit center located at the center of the well, $x_o=0$, and for $x_o=50$, 100, and 150 Å.

$$\mathcal{L} = \vec{\partial}_x \boldsymbol{P} \vec{\partial}_x + \vec{\partial}_x \boldsymbol{Q} + \boldsymbol{Q}^\dagger \vec{\partial}_x + \boldsymbol{R}, \tag{14}$$

where the 8×8 matrices $\boldsymbol{P}$, $\boldsymbol{Q}$, and $\boldsymbol{R}$ can be easily identified from the expressions in the Appendix. The continuity conditions at the interfaces are the continuity of $\boldsymbol{F}(x)$ and of $\boldsymbol{P}(d\boldsymbol{F}/dx)+\boldsymbol{Q}\boldsymbol{F}$, where $\boldsymbol{F}(x)$ is now the eight-component envelope function.[45]

III. NUMERICAL EXAMPLES

In numerical calculations we use the $\mathbf{k}\cdot\mathbf{P}$ band parameters published in our recent tabulation.[48] As concrete examples of our formalism and modeling, we have calculated the energy levels of a $GaAs/Al_{0.3}Ga_{0.7}As$ quantum well and a $GaAs/Al_{0.15}Ga_{0.85}As/Al_{0.3}Ga_{0.7}As$ trilayer superlattice. The choice of these examples is to illustrate the changes in the orbital part of the energy between the Faraday and the Voigt geometries.

A. $GaAs/Al_{0.3}Ga_{0.7}As$ quantum well

We calculate the electronic levels in a $GaAs/Al_{0.3}Ga_{0.7}As$ quantum well structure with a well width of 100 Å. The input parameters for binary GaAs and AlAs used in this calculation are taken from Ref. 48 and the parameters for $Al_xGa_{1-x}As$ are linearly interpolated from the two end binary parameters, except for the energy gap for which a bowing parameter of 0.127 eV is used.

Figure 3 shows the conduction subband energy dispersion both in the Faraday and the Voigt configurations, showing two bound subbands. The quantum numbers in the Faraday

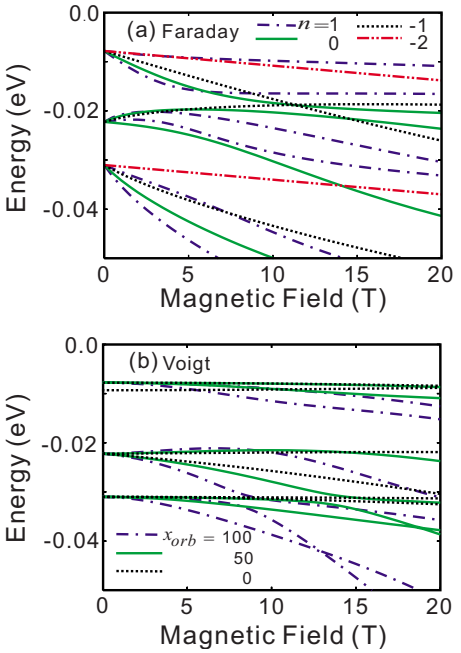

FIG. 4. (Color online) The valence subband dispersion of a 100 Å $GaAs/Al_{0.3}Ga_{0.7}As$ quantum well (a) in the Faraday geometry, with Landau quantum numbers −2, −1, 0, and 1, as indicated on the figure, and (b) in the Voigt geometry for the orbit center located at the center of the well, x_o=0, and for x_o=50, 100, and 150 Å.

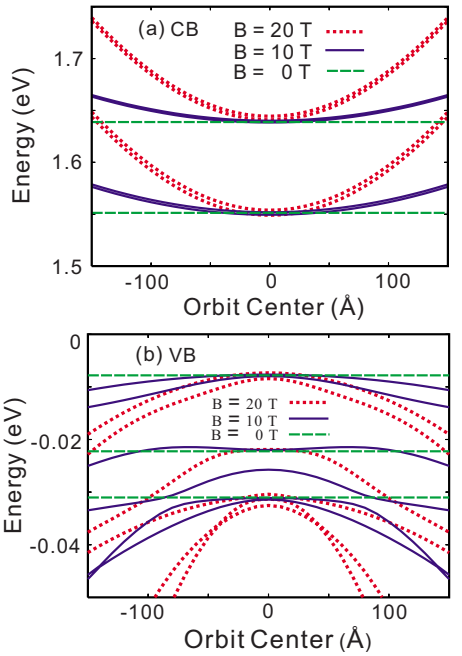

FIG. 5. (Color online) The orbit center dependence is shown for the energy levels of a $GaAs/Al_{0.3}Ga_{0.7}As$ quantum well in the Voigt geometry at B=0, 10, and 20 T, for (a) the conduction band (CB) and (b) the valence band (VB).

geometry are the Landau quantum number n and the wave vector k_y, in a plane perpendicular to the magnetic field, which is implicit and contributes to the degeneracy of the Landau levels. The quantum numbers in the Voigt geometry are the orbit center x_o and the wave vector k_z in the in-plane direction parallel to the magnetic field. Figure 3(a) shows the energy dispersion with respect to the magnetic field in the Faraday geometry for n=−1, 0, 1, and 2, while Fig. 3(b) shows the energy dispersion in the Voigt geometry for x_o =0 (center of the well), 50, 100, and 150 Å with k_z=0. Since the quantum numbers in the Faraday and Voigt geometries are of quite different nature, it is difficult to directly compare these two geometries. A meaningful comparison would be to study the absorption spectra in the two geometries, which we propose to do in a forthcoming paper. One simple observation in Fig. 3 is that the Zeeman splitting is larger in the Voigt geometry. A simple picture of the effect of the magnetic field is to note that it adds a harmonic potential, as illustrated in Fig. 1, and in this picture the subband energy increases with the magnetic field; this is the case with Faraday geometry. But in the case of Voigt geometry with x_o=0, the subband energies decrease over a certain range of the magnetic field, probably due to the interband interaction of our multiband model.

Figure 4 shows the valence subband dispersion in the Faraday configuration with n=−2, −1, 0, and 1 and in the Voigt geometry with x_o=0, 50, and 100 Å with k_z=0, showing two heavy-hole subbands and one light-hole subband. In general, the valence subband structure is very complicated due to intermixing of energy levels.

Figure 5 shows the dependence of energy levels on the location of the orbit center in the Voigt geometry at magnetic fields B=0, 10, and 20 T. As expected, the conduction energy levels increase as the orbit center moves away from the center of the quantum well toward the barrier regions. The behavior of the valence bands is seen as being more complex, again due to the band mixing.

B. $GaAs/Al_{0.15}Ga_{0.85}As/Al_{0.3}Ga_{0.7}As$ trilayer superlattice

It is of interest to study the band structure of multilayered superlattices. A superlattice with more than two composite layers has a structural inversion asymmetry as well, besides the intrinsic inversion asymmetries of the bulk material and the inversion asymmetry arising from the presence of interfaces.[49]

We calculate the energy spectrum of a $GaAs/Al_{0.15}Ga_{0.85}As/Al_{0.3}Ga_{0.7}As$ trilayer superlattice with layer thicknesses 60 Å, 40 Å, and 30 Å, respectively. Unlike in the Faraday geometry, the magnetic field in the Voigt geometry destroys the periodicity of the superlattice, and the usual periodic boundary condition for a superlattice cannot be used. In this calculation, we have employed 13 quantum wells in order to approximate the entire infinite superlattice.

Figure 6 shows the conduction subband dispersion showing two lowest subbands when the orbit center is at the center of the GaAs layer in the central (seventh) quantum well. Since we have 13 wells, each subband has 26 energy levels which correspond to the different superlattice wave vectors before the superlattice periodicity is broken. The lowest level decreases in energy with the magnetic field for a large field, as in the case of a single quantum well. On the other hand, some of the first subband levels grow very rapidly with in-

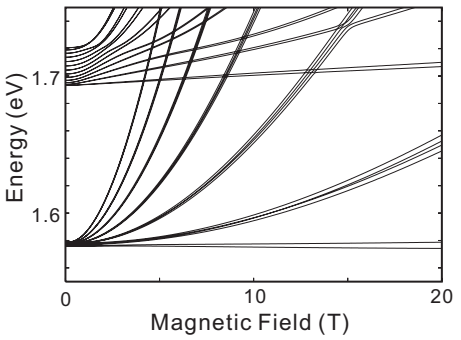

FIG. 6. Conduction subband dispersion of a $GaAs/Al_{0.15}Ga_{0.85}As/Al_{0.3}Ga_{0.7}As$ trilayer superlattice in the Voigt geometry is shown. The magnetic field breaks the translational symmetry of the superlattice; 13 quantum wells were used in the calculations to represent the infinite superlattice.

creasing magnetic field, and they interact with the second subbands. At very low magnetic fields, the system is highly degenerate and numerically unstable; it requires a large number of superlattice periods to capture the Landau orbitals at low fields. As a result, we could not determine the energy levels accurately.

Figure 7 shows the conduction subband energies as a function of the orbit center of the trilayer superlattice at $B=10$ T. The orbit center is moved from the left boundary to the right boundary of the center well, and the periodicity of the energy levels with respect to the orbit center is well determined within the 13-well picture.

IV. CONCLUSIONS

The electronic states in layered zinc-blende semiconductors in the presence of a magnetic field parallel to the layers are explored. The Lagrangian density in the standard eight-band model and continuity conditions across interfaces are derived in the Lagrangian formalism. The Lagrangian is minimized in the framework of the finite element method. As concrete examples of our formalism, band structures of a $GaAs/Al_{0.3}Ga_{0.7}As$ quantum well and a $GaAs/Al_{0.15}Ga_{0.85}As/Al_{0.3}Ga_{0.7}As$ trilayer superlattice were calculated and their features were discussed.

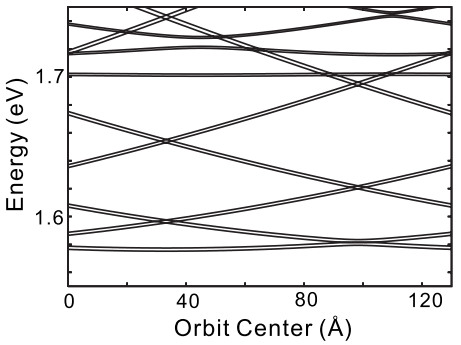

FIG. 7. Conduction subband energies are shown as a function of the orbit center of the trilayer $GaAs/Al_{0.15}Ga_{0.85}As/Al_{0.3}Ga_{0.7}As$ superlattice in the Voigt geometry. The infinite superlattice was represented by 13 quantum wells since the superlattice translational symmetry is broken in the Voigt geometry.

ACKNOWLEDGMENTS

The work at WPI was supported by the National Science Foundation under Grant No. ECS-0725427. The authors wish to thank the Center for Computational Nanoscience at WPI for the use of computing facilities. We wish to thank Quantum Semiconductor Algorithms, Inc., for the use of their finite element and sparse matrix analysis software.

APPENDIX: THE VOIGT LAGRANGIAN IN THE EIGHT-BAND k·P model

We display below for ready reference the 8×8 Lagrangian density in the presence of an in-plane magnetic field $\mathbf{B}=B_o\hat{z}$. The growth direction is chosen to be x direction and the vector potential is chosen to be $\mathbf{A}=B_o x\hat{y}$.

The basis functions are

$$|1\rangle = i|s\rangle\uparrow,$$

$$|2\rangle = i|s\rangle\downarrow,$$

$$|3\rangle = -\left|\frac{x+iy}{\sqrt{2}}\right\rangle\uparrow,$$

$$|4\rangle = -\left|\frac{x+iy}{\sqrt{6}}\right\rangle\downarrow+\left|\frac{2z}{\sqrt{6}}\right\rangle\uparrow,$$

$$|5\rangle = \left|\frac{x-iy}{\sqrt{6}}\right\rangle\uparrow+\left|\frac{2z}{\sqrt{6}}\right\rangle\downarrow,$$

$$|6\rangle = \left|\frac{x-iy}{\sqrt{2}}\right\rangle\downarrow,$$

$$|7\rangle = \left|\frac{x+iy}{\sqrt{3}}\right\rangle\downarrow+\left|\frac{z}{\sqrt{3}}\right\rangle\uparrow,$$

$$|8\rangle = \left|\frac{x-iy}{\sqrt{3}}\right\rangle\uparrow-\left|\frac{z}{\sqrt{3}}\right\rangle\downarrow. \quad \text{(A1)}$$

In the following, standard notations for band parameters are used.[7] Note that $\gamma_i(i=1,2,3)$ in this 8×8 model are the reduced Luttinger parameters, and c_1 and c_2 are given by

$$c_1 = 1+\gamma_1-2\gamma_2-6\gamma_3, \quad c_2 = 1+\gamma_1-2\gamma_2. \quad \text{(A2)}$$

We define two length scales

$$l_o = 1\ \text{Å}, \quad R_o = \sqrt{\frac{\hbar c}{eB_o}}, \quad \text{(A3)}$$

and introduce dimensionless variables

$$x = l_o\tilde{x} = R_o\bar{x}, \quad k_i = \tilde{k}_i/l_o \quad (i=x,y,z). \quad \text{(A4)}$$

Note that there are two different dimensionless variables $\tilde{x}$ and $\bar{x}$ associated with x that are defined above, and should be

distinguished in the following. The following energy scales are also introduced:

$$\mathcal{C} = \frac{\hbar^2}{2m_o l_o^2}, \quad \mathcal{S} = \frac{\hbar^2}{2m_o R_o^2} = \frac{\hbar\omega_B}{2}, \tag{A5}$$

where

$$\omega_B = \frac{eB_o}{m_o c} \tag{A6}$$

is the cyclotron frequency. The orbit center is given by

$$x_o = R_o^2 k_y. \tag{A7}$$

The interband momentum matrix element, **P**, is parametrized in the usual manner and is given by

$$E_p = \frac{2m_0}{\hbar^2}\mathbf{P}^2. \tag{A8}$$

We write the Lagrangian density as $L = \psi^* \mathcal{L} \psi$ with $\mathcal{L}$ as the Lagrangian density operator. The directed derivatives $\overleftarrow{\partial}$ and $\vec{\partial}$ are used here, as described in the main text. The Lagrangian operator in the presence of an in-plane magnetic field is given by

$$\mathcal{L}_{11} = \overleftarrow{\partial}_{\bar{x}} \mathcal{C}(1+2F)\vec{\partial}_{\bar{x}} + \mathcal{S}(1+2F)(\bar{x}+\bar{x}_o)^2 + \mathcal{C}(1+2F)\tilde{k}_z^2 + E_g + \mathcal{S} - E,$$

$$\mathcal{L}_{12} = 0,$$

$$\mathcal{L}_{13} = \overleftarrow{\partial}_{\bar{x}}\left(-\frac{i}{2\sqrt{2}}\sqrt{\mathcal{C}E_p}\right) + \left(\frac{i}{2\sqrt{2}}\sqrt{\mathcal{C}E_p}\right)\vec{\partial}_{\bar{x}} - \frac{i}{\sqrt{2}}\sqrt{\mathcal{S}E_p}(\bar{x}+\bar{x}_o),$$

$$\mathcal{L}_{14} = \sqrt{\frac{2}{3}}\sqrt{\mathcal{C}E_p}\tilde{k}_z,$$

$$\mathcal{L}_{15} = \overleftarrow{\partial}_{\bar{x}}\left(\frac{i}{2\sqrt{6}}\sqrt{\mathcal{C}E_p}\right) + \left(-\frac{i}{2\sqrt{6}}\sqrt{\mathcal{C}E_p}\right)\vec{\partial}_{\bar{x}} + \frac{i}{\sqrt{6}}\sqrt{\mathcal{S}E_p}(\bar{x}+\bar{x}_o),$$

$$\mathcal{L}_{16} = 0,$$

$$\mathcal{L}_{17} = \frac{1}{\sqrt{3}}\sqrt{\mathcal{C}E_p}\tilde{k}_z,$$

$$\mathcal{L}_{18} = \overleftarrow{\partial}_{\bar{x}}\left(\frac{i}{2\sqrt{3}}\sqrt{\mathcal{C}E_p}\right) + \left(-\frac{i}{2\sqrt{3}}\sqrt{\mathcal{C}E_p}\right)\vec{\partial}_{\bar{x}} - \frac{i}{\sqrt{3}}\sqrt{\mathcal{S}E_p}(\bar{x}+\bar{x}_o),$$

$$\mathcal{L}_{21} = 0,$$

$$\mathcal{L}_{22} = \overleftarrow{\partial}_{\bar{x}} \mathcal{C}(1+2F)\vec{\partial}_{\bar{x}} + \mathcal{S}(1+2F)(\bar{x}+\bar{x}_o)^2 + \mathcal{C}(1+2F)\tilde{k}_z^2 + E_g - \mathcal{S} - E,$$

$$\mathcal{L}_{23} = 0,$$

$$\mathcal{L}_{24} = \overleftarrow{\partial}_{\bar{x}}\left(-\frac{i}{2\sqrt{6}}\sqrt{\mathcal{C}E_p}\tilde{k}_z\right) + \left(\frac{i}{2\sqrt{6}}\sqrt{\mathcal{C}E_p}\right)\vec{\partial}_{\bar{x}} - \frac{i}{\sqrt{6}}\sqrt{\mathcal{S}E_p}(\bar{x}+\bar{x}_o),$$

$$\mathcal{L}_{25} = \sqrt{\frac{2}{3}}\sqrt{\mathcal{C}E_p}\tilde{k}_z,$$

$$\mathcal{L}_{26} = \overleftarrow{\partial}_{\bar{x}}\left(\frac{i}{2\sqrt{2}}\sqrt{\mathcal{C}E_p}\right) + \left(-\frac{i}{2\sqrt{2}}\sqrt{\mathcal{C}E_p}\right)\vec{\partial}_{\bar{x}} - \frac{i}{\sqrt{2}}\sqrt{\mathcal{S}E_p}(\bar{x}+\bar{x}_o),$$

$$\mathcal{L}_{27} = \overleftarrow{\partial}_{\bar{x}}\left(\frac{i}{2\sqrt{3}}\sqrt{\mathcal{C}E_p}\right) + \left(-\frac{i}{2\sqrt{3}}\sqrt{\mathcal{C}E_p}\right)\vec{\partial}_{\bar{x}} + \frac{i}{\sqrt{3}}\sqrt{\mathcal{S}E_p}(\bar{x}+\bar{x}_o),$$

$$\mathcal{L}_{28} = -\frac{1}{\sqrt{3}}\sqrt{\mathcal{C}E_p}\tilde{k}_z,$$

$$\mathcal{L}_{31} = \overleftarrow{\partial}_{\bar{x}}\left(-\frac{i}{2\sqrt{2}}\sqrt{\mathcal{C}E_p}\right) + \left(\frac{i}{2\sqrt{2}}\sqrt{\mathcal{C}E_p}\right)\vec{\partial}_{\bar{x}} + \frac{i}{\sqrt{2}}\sqrt{\mathcal{S}E_p}(\bar{x}+\bar{x}_o),$$

$$\mathcal{L}_{32} = 0,$$

$$\mathcal{L}_{33} = \overleftarrow{\partial}_{\bar{x}}[-\mathcal{C}(\gamma_1+\gamma_2)]\vec{\partial}_{\bar{x}} + \overleftarrow{\partial}_{\bar{x}}\left[-\frac{1}{2}\sqrt{\mathcal{C}\mathcal{S}}(c_1+c_2)(\bar{x}+\bar{x}_o)\right] + \left[-\frac{1}{2}\sqrt{\mathcal{C}\mathcal{S}}(c_1+c_2)(\bar{x}+\bar{x}_o)\right]\vec{\partial}_{\bar{x}} - \mathcal{S}(\gamma_1+\gamma_2)(\bar{x}+\bar{x}_o)^2 - \mathcal{C}(\gamma_1-2\gamma_2)\tilde{k}_z^2 - 3\mathcal{S}\left(\kappa+\frac{9}{4}q\right) - E,$$

$$\mathcal{L}_{34} = \overleftarrow{\partial}_{\bar{x}}\left(-\frac{i}{\sqrt{3}}\mathcal{C}c_1\tilde{k}_z\right) + \left(-\frac{i}{\sqrt{3}}\mathcal{C}c_2\tilde{k}_z\right)\vec{\partial}_{\bar{x}} - 2\sqrt{3}i\sqrt{\mathcal{C}\mathcal{S}}\gamma_3(\bar{x}+\bar{x}_o)\tilde{k}_z,$$

$$\mathcal{L}_{35} = \overleftarrow{\partial}_{\bar{x}}(\sqrt{3}\mathcal{C}\gamma_2)\vec{\partial}_{\bar{x}} + \overleftarrow{\partial}_{\bar{x}}[\sqrt{3}\sqrt{\mathcal{C}\mathcal{S}}\gamma_3(\bar{x}+\bar{x}_o)] + [-\sqrt{3}\sqrt{\mathcal{C}\mathcal{S}}\gamma_3(\bar{x}+\bar{x}_o)]\vec{\partial}_{\bar{x}} - \sqrt{3}\mathcal{S}\gamma_2(\bar{x}+\bar{x}_o)^2,$$

$$\mathcal{L}_{36} = 0,$$

$$\mathcal{L}_{37} = \overleftarrow{\partial}_{\bar{x}}\left(-\frac{i}{\sqrt{6}}\mathcal{C}c_1\tilde{k}_z\right) + \left(-\frac{i}{\sqrt{6}}\mathcal{C}c_2\tilde{k}_z\right)\vec{\partial}_{\bar{x}} - i\sqrt{6}\sqrt{\mathcal{C}\mathcal{S}}\gamma_3(\bar{x}+\bar{x}_o)\tilde{k}_z,$$

$$\mathcal{L}_{38} = \overleftarrow{\partial}_{\bar{x}}(\sqrt{6}\mathcal{C}\gamma_2)\vec{\partial}_{\bar{x}} + \overleftarrow{\partial}_{\bar{x}}[\sqrt{6}\sqrt{\mathcal{C}\mathcal{S}}\gamma_3(\bar{x}+\bar{x}_o)] + [-\sqrt{6}\sqrt{\mathcal{C}\mathcal{S}}\gamma_3(\bar{x}+\bar{x}_o)]\vec{\partial}_{\bar{x}} - \sqrt{6}\mathcal{S}\gamma_2(\bar{x}+\bar{x}_o)^2,$$

$$\mathcal{L}_{41} = \sqrt{\frac{2}{3}}\sqrt{\mathcal{C}E_p}\tilde{k}_z,$$

$$\mathcal{L}_{42} = \overleftarrow{\partial}_{\bar{x}}\left(-\frac{i}{2\sqrt{6}}\sqrt{\mathcal{C}E_p}\right) + \left(\frac{i}{2\sqrt{6}}\sqrt{\mathcal{C}E_p}\right)\vec{\partial}_{\bar{x}} + \frac{i}{\sqrt{6}}\sqrt{\mathcal{S}E_p}(\bar{x}+\bar{x}_o),$$

$$\mathcal{L}_{43} = \overleftarrow{\partial}_{\bar{x}}\left(\frac{i}{\sqrt{3}}\mathcal{C}c_2\tilde{k}_z\right) + \left(\frac{i}{\sqrt{3}}\mathcal{C}c_1\tilde{k}_z\right)\vec{\partial}_{\bar{x}} + 2\sqrt{3}i\sqrt{\mathcal{C}\mathcal{S}}\gamma_3(\bar{x}+\bar{x}_o)\tilde{k}_z,$$

$$\begin{aligned}\mathcal{L}_{44} = {} & \overleftarrow{\partial}_{\bar{x}}[-\mathcal{C}(\gamma_1-\gamma_2)]\vec{\partial}_{\bar{x}} + \overleftarrow{\partial}_{\bar{x}}\left[-\frac{1}{6}\sqrt{\mathcal{C}\mathcal{S}}(c_1+c_2)(\bar{x}+\bar{x}_o)\right] \\ & + \left[-\frac{1}{6}\sqrt{\mathcal{C}\mathcal{S}}(c_1+c_2)(\bar{x}+\bar{x}_o)\right]\vec{\partial}_{\bar{x}} - \mathcal{S}(\gamma_1-\gamma_2)(\bar{x}+\bar{x}_o)^2 \\ & - \mathcal{C}(\gamma_1+2\gamma_2)\tilde{k}_z^2 - \mathcal{S}\left(\kappa+\frac{1}{4}q\right) - E,\end{aligned}$$

$$\mathcal{L}_{45} = \overleftarrow{\partial}_{\bar{x}}\left[-\frac{i}{3}\mathcal{C}(c_1+c_2)\tilde{k}_z\right] + \left[-\frac{i}{3}\mathcal{C}(c_1+c_2)\tilde{k}_z\right]\vec{\partial}_{\bar{x}},$$

$$\begin{aligned}\mathcal{L}_{46} = {} & \overleftarrow{\partial}_{\bar{x}}(\sqrt{3}\mathcal{C}\gamma_2)\vec{\partial}_{\bar{x}} + \overleftarrow{\partial}_{\bar{x}}[\sqrt{3}\sqrt{\mathcal{C}\mathcal{S}}\gamma_3(\bar{x}+\bar{x}_o)] \\ & + [-\sqrt{3}\sqrt{\mathcal{C}\mathcal{S}}\gamma_3(\bar{x}+\bar{x}_o)]\vec{\partial}_{\bar{x}} - \sqrt{3}\mathcal{S}\gamma_2(\bar{x}+\bar{x}_o)^2,\end{aligned}$$

$$\begin{aligned}\mathcal{L}_{47} = {} & \overleftarrow{\partial}_{\bar{x}}(\sqrt{2}\mathcal{C}\gamma_2)\vec{\partial}_{\bar{x}} + \overleftarrow{\partial}_{\bar{x}}\left[\frac{1}{3\sqrt{2}}\sqrt{\mathcal{C}\mathcal{S}}(c_1+c_2)(\bar{x}+\bar{x}_o)\right] \\ & + \left[\frac{1}{3\sqrt{2}}\sqrt{\mathcal{C}\mathcal{S}}(c_1+c_2)(\bar{x}+\bar{x}_o)\right]\vec{\partial}_{\bar{x}} + \sqrt{2}\mathcal{S}\gamma_2(\bar{x}+\bar{x}_o)^2 \\ & - 2\sqrt{2}\mathcal{C}\gamma_2\tilde{k}_z^2 + \sqrt{2}\mathcal{S}(\kappa+1),\end{aligned}$$

$$\begin{aligned}\mathcal{L}_{48} = {} & \overleftarrow{\partial}_{\bar{x}}\left[\frac{i}{3\sqrt{2}}\mathcal{C}(c_1-2c_2)\tilde{k}_z\right] + \left[-\frac{i}{3\sqrt{2}}\mathcal{C}(2c_1-c_2)\tilde{k}_z\right]\vec{\partial}_{\bar{x}} \\ & + 3\sqrt{2}i\sqrt{\mathcal{C}\mathcal{S}}\gamma_3(\bar{x}+\bar{x}_o)\tilde{k}_z,\end{aligned}$$

$$\mathcal{L}_{51} = \overleftarrow{\partial}_{\bar{x}}\left(\frac{i}{2\sqrt{6}}\sqrt{\mathcal{C}E_p}\right) + \left(-\frac{i}{2\sqrt{6}}\sqrt{\mathcal{C}E_p}\right)\vec{\partial}_{\bar{x}} - \frac{i}{\sqrt{6}}\sqrt{\mathcal{S}E_p}(\bar{x}+\bar{x}_o),$$

$$\mathcal{L}_{52} = \sqrt{\frac{2}{3}}\sqrt{\mathcal{C}E_p}\tilde{k}_z,$$

$$\begin{aligned}\mathcal{L}_{53} = {} & \overleftarrow{\partial}_{\bar{x}}(\sqrt{3}\mathcal{C}\gamma_2)\vec{\partial}_{\bar{x}} + \overleftarrow{\partial}_{\bar{x}}[-\sqrt{3}\sqrt{\mathcal{C}\mathcal{S}}\gamma_3(\bar{x}+\bar{x}_o)] \\ & + [\sqrt{3}\sqrt{\mathcal{C}\mathcal{S}}\gamma_3(\bar{x}+\bar{x}_o)]\vec{\partial}_{\bar{x}} - \sqrt{3}\mathcal{S}\gamma_2(\bar{x}+\bar{x}_o)^2,\end{aligned}$$

$$\mathcal{L}_{54} = \overleftarrow{\partial}_{\bar{x}}\left[\frac{i}{3}\mathcal{C}(c_1+c_2)\tilde{k}_z\right] + \left[\frac{i}{3}\mathcal{C}(c_1+c_2)\tilde{k}_z\right]\vec{\partial}_{\bar{x}},$$

$$\begin{aligned}\mathcal{L}_{55} = {} & \overleftarrow{\partial}_{\bar{x}}[-\mathcal{C}(\gamma_1-\gamma_2)]\vec{\partial}_{\bar{x}} + \overleftarrow{\partial}_{\bar{x}}\left[\frac{1}{6}\sqrt{\mathcal{C}\mathcal{S}}(c_1+c_2)(\bar{x}+\bar{x}_o)\right] \\ & + \left[\frac{1}{6}\sqrt{\mathcal{C}\mathcal{S}}(c_1+c_2)(\bar{x}+\bar{x}_o)\right]\vec{\partial}_{\bar{x}} - \mathcal{S}(\gamma_1-\gamma_2)(\bar{x}+\bar{x}_o)^2 \\ & - \mathcal{C}(\gamma_1+2\gamma_2)\tilde{k}_z^2 + \mathcal{S}\left(\kappa+\frac{1}{4}q\right) - E,\end{aligned}$$

$$\begin{aligned}\mathcal{L}_{56} = {} & \overleftarrow{\partial}_{\bar{x}}\left[-\frac{i}{\sqrt{3}}\mathcal{C}c_2\tilde{k}_z\right] + \left[-\frac{i}{\sqrt{3}}\mathcal{C}c_1\tilde{k}_z\right]\vec{\partial}_{\bar{x}} \\ & + 2\sqrt{3}i\sqrt{\mathcal{C}\mathcal{S}}\gamma_3(\bar{x}+\bar{x}_o)\tilde{k}_z,\end{aligned}$$

$$\begin{aligned}\mathcal{L}_{57} = {} & \overleftarrow{\partial}_{\bar{x}}\left[\frac{i}{3\sqrt{2}}\mathcal{C}(c_1-2c_2)\tilde{k}_z\right] + \left[-\frac{i}{3\sqrt{2}}\mathcal{C}(2c_1-c_2)\tilde{k}_z\right]\vec{\partial}_{\bar{x}} \\ & - 3\sqrt{2}i\sqrt{\mathcal{C}\mathcal{S}}\gamma_3(\bar{x}+\bar{x}_o)\tilde{k}_z,\end{aligned}$$

$$\begin{aligned}\mathcal{L}_{58} = {} & \overleftarrow{\partial}_{\bar{x}}(-\sqrt{2}\mathcal{C}\gamma_2)\vec{\partial}_{\bar{x}} + \overleftarrow{\partial}_{\bar{x}}\left[\frac{1}{3\sqrt{2}}\sqrt{\mathcal{C}\mathcal{S}}(c_1+c_2)(\bar{x}+\bar{x}_o)\right] \\ & + \left[\frac{1}{3\sqrt{2}}\sqrt{\mathcal{C}\mathcal{S}}(c_1+c_2)(\bar{x}+\bar{x}_o)\right]\vec{\partial}_{\bar{x}} - \sqrt{2}\mathcal{S}\gamma_2(\bar{x}+\bar{x}_o)^2 \\ & + 2\sqrt{2}\mathcal{C}\gamma_2\tilde{k}_z^2 + \sqrt{2}\mathcal{S}(\kappa+1),\end{aligned}$$

$$\mathcal{L}_{61} = 0,$$

$$\mathcal{L}_{62} = \overleftarrow{\partial}_{\bar{x}}\left(\frac{i}{2\sqrt{2}}\sqrt{\mathcal{C}E_p}\right) + \left(-\frac{i}{2\sqrt{2}}\sqrt{\mathcal{C}E_p}\right)\vec{\partial}_{\bar{x}} + \frac{i}{\sqrt{2}}\sqrt{\mathcal{S}E_p}(\bar{x}+\bar{x}_o),$$

$$\mathcal{L}_{63} = 0,$$

$$\begin{aligned}\mathcal{L}_{64} = {} & \overleftarrow{\partial}_{\bar{x}}(\sqrt{3}\mathcal{C}\gamma_2)\vec{\partial}_{\bar{x}} + \overleftarrow{\partial}_{\bar{x}}[-\sqrt{3}\sqrt{\mathcal{C}\mathcal{S}}\gamma_3(\bar{x}+\bar{x}_o)] \\ & + [\sqrt{3}\sqrt{\mathcal{C}\mathcal{S}}\gamma_3(\bar{x}+\bar{x}_o)]\vec{\partial}_{\bar{x}} - \mathcal{S}(\sqrt{3}\gamma_2)(\bar{x}+\bar{x}_o)^2,\end{aligned}$$

$$\mathcal{L}_{65} = \overleftarrow{\partial}_{\bar{x}}\left(\frac{i}{\sqrt{3}}\mathcal{C}c_1\tilde{k}_z\right) + \left(\frac{i}{\sqrt{3}}\mathcal{C}c_2\tilde{k}_z\right)\vec{\partial}_{\bar{x}} - 2\sqrt{3}i\sqrt{\mathcal{C}\mathcal{S}}\gamma_3(\bar{x}+\bar{x}_o)\tilde{k}_z,$$

$$\begin{aligned}\mathcal{L}_{66} = {} & \overleftarrow{\partial}_{\bar{x}}[-\mathcal{C}(\gamma_1+\gamma_2)]\vec{\partial}_{\bar{x}} + \overleftarrow{\partial}_{\bar{x}}\left[\frac{1}{2}\sqrt{\mathcal{C}\mathcal{S}}(c_1+c_2)(\bar{x}+\bar{x}_o)\right] \\ & + \left[\frac{1}{2}\sqrt{\mathcal{C}\mathcal{S}}(c_1+c_2)(\bar{x}+\bar{x}_o)\right]\vec{\partial}_{\bar{x}} - \mathcal{S}(\gamma_1+\gamma_2)(\bar{x}+\bar{x}_o)^2 \\ & - \mathcal{C}(\gamma_1-2\gamma_2)\tilde{k}_z^2 + 3\mathcal{S}\left(\kappa+\frac{9}{4}q\right) - E,\end{aligned}$$

$$\begin{aligned}\mathcal{L}_{67} = {} & \overleftarrow{\partial}_{\bar{x}}(-\sqrt{6}\mathcal{C}\gamma_2)\vec{\partial}_{\bar{x}} + \overleftarrow{\partial}_{\bar{x}}[\sqrt{6}\sqrt{\mathcal{C}\mathcal{S}}\gamma_3(\bar{x}+\bar{x}_o)] \\ & + [-\sqrt{6}\sqrt{\mathcal{C}\mathcal{S}}\gamma_3(\bar{x}+\bar{x}_o)]\vec{\partial}_{\bar{x}} + \sqrt{6}\mathcal{S}\gamma_2(\bar{x}+\bar{x}_o)^2,\end{aligned}$$

$$\begin{aligned}\mathcal{L}_{68} = {} & \overleftarrow{\partial}_{\bar{x}}\left(-\frac{i}{\sqrt{6}}\mathcal{C}c_1\tilde{k}_z\right) + \left(-\frac{i}{\sqrt{6}}\mathcal{C}c_2\tilde{k}_z\right)\vec{\partial}_{\bar{x}} \\ & + i\sqrt{6}\sqrt{\mathcal{C}\mathcal{S}}\gamma_3(\bar{x}+\bar{x}_o)\tilde{k}_z,\end{aligned}$$

$$\mathcal{L}_{71} = \frac{1}{\sqrt{3}}\sqrt{\mathcal{C}E_p}\tilde{k}_z,$$

$$\mathcal{L}_{72} = \overleftarrow{\partial}_{\bar{x}}\left(\frac{i}{2\sqrt{3}}\sqrt{\mathcal{C}E_p}\right) + \left(-\frac{i}{2\sqrt{3}}\sqrt{\mathcal{C}E_p}\right)\vec{\partial}_{\bar{x}} - \frac{i}{\sqrt{3}}\sqrt{\mathcal{S}E_p}(\bar{x}+\bar{x}_o),$$

$$\mathcal{L}_{73} = \overleftarrow{\partial}_{\tilde{x}}\left(\frac{i}{\sqrt{6}}\mathcal{C}c_2\tilde{k}_z\right) + \left(\frac{i}{\sqrt{6}}\mathcal{C}c_1\tilde{k}_z\right)\vec{\partial}_{\tilde{x}} + i\sqrt{6}\sqrt{\mathcal{CS}}\gamma_3(\bar{x}+\bar{x}_o)\tilde{k}_z,$$

$$\mathcal{L}_{74} = \overleftarrow{\partial}_{\tilde{x}}(\sqrt{2}\mathcal{C}\gamma_2)\vec{\partial}_{\tilde{x}} + \overleftarrow{\partial}_{\tilde{x}}\left[\frac{1}{3\sqrt{2}}\sqrt{\mathcal{CS}}(c_1+c_2)(\bar{x}+\bar{x}_o)\right] + \left[\frac{1}{3\sqrt{2}}\sqrt{\mathcal{CS}}(c_1+c_2)(\bar{x}+\bar{x}_o)\right]\vec{\partial}_{\tilde{x}} + \sqrt{2}\mathcal{S}\gamma_2(\bar{x}+\bar{x}_o)^2 - 2\sqrt{2}\mathcal{C}\gamma_2\tilde{k}_z^2 + \sqrt{2}\mathcal{S}(\kappa+1),$$

$$\mathcal{L}_{75} = \overleftarrow{\partial}_{\tilde{x}}\left[\frac{i}{3\sqrt{2}}\mathcal{C}(2c_1-c_2)\tilde{k}_z\right] + \left[-\frac{i}{3\sqrt{2}}\mathcal{C}(c_1-2c_2)\tilde{k}_z\right]\vec{\partial}_{\tilde{x}} + 3\sqrt{2}i\sqrt{\mathcal{CS}}\gamma_3\tilde{k}_z(\bar{x}+\bar{x}_o),$$

$$\mathcal{L}_{76} = \overleftarrow{\partial}_{\tilde{x}}(-\sqrt{6}\mathcal{C}\gamma_2)\vec{\partial}_{\tilde{x}} + \overleftarrow{\partial}_{\tilde{x}}[-\sqrt{6}\sqrt{\mathcal{CS}}\gamma_3(\bar{x}+\bar{x}_o)] + [\sqrt{6}\sqrt{\mathcal{CS}}\gamma_3(\bar{x}+\bar{x}_o)]\vec{\partial}_{\tilde{x}} + \sqrt{6}\mathcal{S}\gamma_2(\bar{x}+\bar{x}_o)^2,$$

$$\mathcal{L}_{77} = \overleftarrow{\partial}_{\tilde{x}}(-\mathcal{C}\gamma_1)\vec{\partial}_{\tilde{x}} + \overleftarrow{\partial}_{\tilde{x}}\left[-\frac{1}{3}\sqrt{\mathcal{CS}}(c_1+c_2)(\bar{x}+\bar{x}_o)\right] + \left[-\frac{1}{3}\sqrt{\mathcal{CS}}(c_1+c_2)(\bar{x}+\bar{x}_o)\right]\vec{\partial}_{\tilde{x}} - \mathcal{S}\gamma_1(\bar{x}+\bar{x}_o)^2 - \mathcal{C}\gamma_1\tilde{k}_z^2 - \Delta - \mathcal{S}(2\kappa+1) - E,$$

$$\mathcal{L}_{78} = \overleftarrow{\partial}_{\tilde{x}}\left[-\frac{i}{3}\mathcal{C}(c_1+c_2)\tilde{k}_z\right] + \left[-\frac{i}{3}\mathcal{C}(c_1+c_2)\tilde{k}_z\right]\vec{\partial}_{\tilde{x}},$$

$$\mathcal{L}_{81} = \overleftarrow{\partial}_{\tilde{x}}\left(\frac{i}{2\sqrt{3}}\sqrt{\mathcal{C}E_p}\right) + \left(-\frac{i}{2\sqrt{3}}\sqrt{\mathcal{C}E_p}\right)\vec{\partial}_{\tilde{x}} + \frac{i}{\sqrt{3}}\sqrt{\mathcal{S}E_p}(\bar{x}+\bar{x}_o),$$

$$\mathcal{L}_{82} = -\frac{1}{\sqrt{3}}\sqrt{\mathcal{C}E_p}\tilde{k}_z,$$

$$\mathcal{L}_{83} = \overleftarrow{\partial}_{\tilde{x}}(\sqrt{6}\mathcal{C}\gamma_2)\vec{\partial}_{\tilde{x}} + \overleftarrow{\partial}_{\tilde{x}}[-\sqrt{6}\sqrt{\mathcal{CS}}\gamma_3(\bar{x}+\bar{x}_o)] + [\sqrt{6}\sqrt{\mathcal{CS}}\gamma_3(\bar{x}+\bar{x}_o)]\vec{\partial}_{\tilde{x}} - \sqrt{6}\mathcal{S}\gamma_2(\bar{x}+\bar{x}_o)^2,$$

$$\mathcal{L}_{84} = \overleftarrow{\partial}_{\tilde{x}}\left[\frac{i}{3\sqrt{2}}\mathcal{C}(2c_1-c_2)\tilde{k}_z\right] + \left[-\frac{i}{3\sqrt{2}}\mathcal{C}(c_1-2c_2)\tilde{k}_z\right]\vec{\partial}_{\tilde{x}} - 3\sqrt{2}i\sqrt{\mathcal{CS}}\gamma_3(\bar{x}+\bar{x}_o)\tilde{k}_z,$$

$$\mathcal{L}_{85} = \overleftarrow{\partial}_{\tilde{x}}(-\sqrt{2}\mathcal{C}\gamma_2)\vec{\partial}_{\tilde{x}} + \overleftarrow{\partial}_{\tilde{x}}\left[\frac{1}{3\sqrt{2}}\sqrt{\mathcal{CS}}(c_1+c_2)(\bar{x}+\bar{x}_o)\right] + \left[\frac{1}{3\sqrt{2}}\sqrt{\mathcal{CS}}(c_1+c_2)(\bar{x}+\bar{x}_o)\right]\vec{\partial}_{\tilde{x}} - \sqrt{2}\mathcal{S}\gamma_2(\bar{x}+\bar{x}_o)^2 + 2\sqrt{2}\mathcal{C}\gamma_2\tilde{k}_z^2 + \sqrt{2}\mathcal{S}(\kappa+1),$$

$$\mathcal{L}_{86} = \overleftarrow{\partial}_{\tilde{x}}\left[\frac{i}{\sqrt{6}}\mathcal{C}c_2\tilde{k}_z\right] + \left[\frac{i}{\sqrt{6}}\mathcal{C}c_1\tilde{k}_z\right]\vec{\partial}_{\tilde{x}} - i\sqrt{6}\sqrt{\mathcal{CS}}\gamma_3(\bar{x}+\bar{x}_o)\tilde{k}_z,$$

$$\mathcal{L}_{87} = \overleftarrow{\partial}_{\tilde{x}}\left[\frac{i}{3}\mathcal{C}(c_1+c_2)\tilde{k}_z\right] + \left[\frac{i}{3}\mathcal{C}(c_1+c_2)\tilde{k}_z\right]\vec{\partial}_{\tilde{x}},$$

$$\mathcal{L}_{88} = \overleftarrow{\partial}_{\tilde{x}}(-\mathcal{C}\gamma_1)\vec{\partial}_{\tilde{x}} + \overleftarrow{\partial}_{\tilde{x}}\left[\frac{1}{3}\sqrt{\mathcal{CS}}(c_1+c_2)(\bar{x}+\bar{x}_o)\right] + \left[\frac{1}{3}\sqrt{\mathcal{CS}}(c_1+c_2)(\bar{x}+\bar{x}_o)\right]\vec{\partial}_{\tilde{x}} - \mathcal{S}\gamma_1(\bar{x}+\bar{x}_o)^2 - \mathcal{C}\gamma_1\tilde{k}_z^2 - \Delta + \mathcal{S}(2\kappa+1) - E.$$

*khyoo@khu.ac.kr

[1] L. D. Landau and E. M. Lifshitz, *Quantum Mechanics: Non-Relativistic Theory*, 3rd ed. (Elsevier Science, Burlington, MA, 2003).

[2] G. Dresselhaus, A. F. Kip, and C. Kittel, Phys. Rev. **98**, 368 (1955).

[3] R. N. Dexter, H. J. Zieger, and B. Lax, Phys. Rev. **104**, 637 (1956).

[4] E. Burstein and G. S. Picus, Phys. Rev. **105**, 1123 (1957).

[5] S. Zwerdling and B. Lax, Phys. Rev. **106**, 51 (1957); S. Zwerdling, B. Lax, and L. M. Roth, *ibid.* **108**, 1402 (1957); S. Zwerdling, L. M. Roth, and B. Lax, *ibid.* **109**, 2207 (1958); S. Zwerdling, B. Lax, L. M. Roth, and K. J. Button, *ibid.* **114**, 80 (1959); L. M. Roth, B. Lax, and S. Zwerdling, *ibid.* **114**, 90 (1959).

[6] C. R. Pidgeon and R. N. Brown, Phys. Rev. **146**, 575 (1966).

[7] M. H. Weiler, in *Semiconductors and Semimetals*, edited by R. K. Willardson and A. C. Beer (Academic, New York, 1981), Vol. 16, p. 119.

[8] G. Lommer, F. Malcher, and U. Rossler, Phys. Rev. B **32**, 6965 (1985).

[9] R. L. Aggarwal, in *Semiconductors and Semimetals*, edited by R. K. Willardson and A. C. Beer (Academic, New York, 1972), Vol. 9, p. 151.

[10] J. M. Luttinger, Phys. Rev. **102**, 1030 (1956).

[11] J. M. Luttinger and W. Kohn, Phys. Rev. **97**, 869 (1955).

[12] S. R. White and L. J. Sham, Phys. Rev. Lett. **47**, 879 (1981).

[13] D. A. Broido and L. J. Sham, Phys. Rev. B **31**, 888 (1985).

[14] S. Lamari and L. J. Sham, Phys. Rev. B **38**, 9810 (1988).

[15] M. Altarelli, in *Applications of High Magnetic Fields in Semiconductor Physics*, edited by G. Landwehr (Springer, Berlin, 1983), p. 174; Phys. Rev. B **28**, 842 (1983).

[16] L. R. Ram-Mohan, K. H. Yoo, and R. L. Aggarwal, Phys. Rev. B **38**, 6151 (1988).

[17] K. H. Yoo, R. L. Aggarwal, and L. R. Ram-Mohan, J. Vac. Sci. Technol. A **7**, 415 (1989).

[18] B. Chen, M. Lazzouni, and L. R. Ram-Mohan, Phys. Rev. B **45**, 1204 (1992).

[19] M. Dobrowolska, T. Wojtowicz, H. Luo, J. K. Furdyna, O. K. Wu, J. R. Meyer, C. A. Hoffman, F. J. Bartoli, and L. R. Ram-

Mohan, Semicond. Sci. Technol. **5**, s103 (1990).
[20] J. R. Meyer, R. J. Wagner, F. J. Bartoli, C. A. Hoffman, M. Dobrowolska, T. Wojtowicz, J. K. Furdyna, and L. R. Ram-Mohan, Phys. Rev. B **42**, 9050 (1990).
[21] N. F. Johnson, P. M. Hui, and H. Ehrenreich, Phys. Rev. Lett. **61**, 1993 (1988).
[22] E. O. Kane, J. Phys. Chem. Solids **6**, 236 (1958); E. O. Kane, in *Semiconductors and Semimetals*, edited by R. K. Willardson and A. C. Beer (Academic, New York, 1966), Vol. 1, p. 75; E. O. Kane, in *Handbook on Semiconductors*, edited by W. Paul (North-Holland, Amsterdam, 1982), Vol. 1, p. 193.
[23] G. Bastard, Phys. Rev. B **24**, 5693 (1981).
[24] G. Bastard, Phys. Rev. B **25**, 7584 (1982).
[25] G. Bastard, *Wave Mechanics Applied to Semiconductor Heterostructures* (Les Editions de Physique, Les Ulis, France, 1988).
[26] L. R. Ram-Mohan, *Finite Element and Boundary Element Applications to Quantum Mechanics* (Oxford University Press, Oxford, 2002).
[27] O. C. Zienkiewicz, *The Finite Element Method* (McGraw-Hill, New York, 1989); O. C. Zienkiewicz and R. L. Taylor, *The Finite Element Method* (McGraw-Hill, New York, 1994).
[28] B. G. Galerkin, Vestn. Inzh. Tekh. **19**, 897 (1915).
[29] T. J. R. Hughes, *The Finite Element Method: Linear Static and Dynamic Finite Element Analysis* (Prentice-Hall, Englewood Cliffs, NJ, 1987); T. J. R. Hughes, *The Finite Element Method: Linear Static and Dynamic Finite Element Analysis* (Dover, New York, NY, 2000).
[30] H. R. Schwarz, *Finite Element Methods* (Academic, New York, 1988).
[31] K.-J. Bathe, *Finite Element Procedures in Engineering Analysis* (Prentice-Hall, New Jersey, 1982).
[32] G. Belle, J. C. Maan, and G. Weimann, Solid State Commun. **56**, 65 (1985).
[33] G. Belle, J. C. Maan, and G. Weimann, Surf. Sci. **170**, 611 (1986).
[34] J. C. Maan, Superlattices Microstruct. **2**, 557 (1986).
[35] J. C. Maan, in *Two-Dimensional Systems, Heterostructures, and Superlattices*, Springer Series in Solid State Sciences Vol. 53, edited by G. Bauer, F. Kuchar, and H. Heinrich (Springer, Berlin, 1984), p. 183.
[36] J. B. Xia and W. J. Fan, Phys. Rev. B **40**, 8508 (1989).
[37] J. B. Xia and K. Huang, Phys. Rev. B **42**, 11884 (1990).
[38] M. Altarelli and G. Platero, Surf. Sci. **196**, 540 (1988).
[39] M. Altarelli, in *Interfaces, Quantum Wells, and Superlattices*, NATO Advanced Studies Institute, Series B Vol. 179, edited by C. R. Leavens and R. Taylor (Plenum, New York, 1988), p. 43.
[40] G. Platero and M. Altarelli, Phys. Rev. B **39**, 3758 (1989).
[41] P. O. Löwdin, J. Chem. Phys. **19**, 1396 (1951).
[42] W. H. Press, S. A. Teukolsky, W. T. Vetterling, and B. R. Flannery, *Numerical Recipes* (Cambridge University Press, Cambridge, 1992).
[43] C. Lanczos, J. Res. NBS **45**, 255 (1950); W. E. Arnoldi, Q. Appl. Math. **9**, 17 (1951).
[44] M. Gell-Mann and M. Levy, Il Nuov. Cim. **16**, 705 (1960); also see, J. Schwinger, Phys. Rev. **91**, 713 (1953).
[45] L. R. Ram-Mohan and K.-H. Yoo, J. Phys.: Condens. Matter **18**, R901 (2006).
[46] M. G. Burt, Semicond. Sci. Technol. **2**, 460 (1987); J. Phys.: Condens. Matter **4**, 6651 (1992).
[47] B. A. Foreman, Phys. Rev. B **48**, 4964 (1993).
[48] I. Vurgaftman, J. R. Meyer, and L. R. Ram-Mohan, J. Appl. Phys. **89**, 5815 (2001).
[49] L. C. Lew Yan Voon and L. R. Ram-Mohan, *Proceedings of Seventh Annual IEEE Lasers and Electro-Optic Society Meeting, Vol. 1* (IEEE, Boston, 1994), pp. 30–31.